ISSN 1392–1320 MATERIALS SCIENCE (MEDŽIAGOTYRA). Vol. 11, No. 3. 2005

The Role of Grain Boundaries in the Mechanism of Plasma Immersion Hydrogenation of Nanocrystalline Mg Films

Darius MILČIUS[1*], Liudas PRANEVIČIUS[1,2], Birutė BOBROVAITĖ[2], Irmantas BARNACKAS[2]

[1] *Material Research and Testing Laboratory*, *Lithuanian Energy Institute, Breslaujos 3, LT-44403 Kaunas, Lithuania*
[2] *Physics Department*, *Vytautas Magnus University, Vileikos 8, LT-44404, Kaunas, Lithuania*

Received 15 May 2005; accepted 09 June 2005

In this paper, attention is focused on the nanostructured magnesium films for hydrogen storage. It is shown that 2 μm-thick Mg film is transformed into MgH_2 film under high-flux and fluence hydrogen plasma immersion ion implantation at 450 K for 35 min. All hydrogen desorbs at temperature about 530 K, which corresponds to the decomposition of $MgH_2 \rightarrow Mg + H_2\uparrow$. The macroscopic and microscopic observations show that magnesium film undergoes a high deformation during hydrogenation-dehydrogenation reaction. The suggested hydrogenation model is based upon the incorporation of excess of hydrogen atoms in grain boundaries of nanocrystalline Mg film driven by the increase in surface chemical potential associated with the implantation flux. The results provide new aspects of hydriding of thin nanocrystalline film materials under highly non-equilibrium conditions on the surface.
Keywords: hydrogenation, Mg film, grain boundaries, plasma immersion ion implantation.

INTRODUCTION

Search for materials to store hydrogen in hydride forming systems is the subject of research for several decades. Nanostructured materials are distinguished from conventional polycrystalline materials by the large fraction of grain boundaries in bulk materials, and hence the amount of atom located within of close to grain boundaries is of the same order as in the bulk. Surface properties start to determine bulk properties and noteworthy, that monolayers further away from the internal surfaces experience modified conditions [1]. Clearly, the interaction between bulk properties of the material and its free surface and internal surfaces is critical. Modern technologies allow tailoring and manipulation of fundamental material properties by decreasing the length scale to the nanoscale [1].

In this paper, attention will be focused on the nanostructured magnesium films used for hydrogen storage. Magnesium is of interest as a possible hydrogen storage material because of its high hydrogen storage capacity (MgH_2 corresponds to 7.6 wt.% H). However, pure magnesium metal has poor hydrogenation characteristics: the kinetics of hydrogenation–dehydrogenation is very slow and the reaction occurs only at very high temperature [2].

Various attempts have been undertaken to improve the kinetics of magnesium by modifying surface, reducing the particle size of powder, controlling the surface oxidation or adding various elements [3 – 5]. Energetic ball milling of nanocrystalline magnesium hydride resulted in greatly improved hydrogen sorption kinetics [6]. However, no general mechanism for the hydriding–dehydriding reaction has been proposed despite the existence of a considerable body of experimental data.

In the present work, we study hydrogen absorption–desorption properties of nanocrystalline magnesium films in order to understand the hydriding reaction kinetics. We investigate magnesium films prepared by unbalanced magnetron sputter deposition technique enabling to modify the microstructure of deposited film. The plasma immersion hydrogen ion implantation technique is used for hydrogenation of magnesium film.

An attempt to understand the mechanism driving hydrogen into the bulk of film and out of it is made on the basis of the model based on the assumption that the surface of the film during hydrogenation is at a higher chemical potential than the static surface. This chemical potential difference of the free surface relative to the grain boundary is the driving force for the movement of atoms into the grain boundaries of nanocrystalline film and the creation of compressive stress. Dislocation plasticity within the nanograins and diffusional flow of hydrogen between the grain boundaries and the free surface provide mechanisms for hydrogenation kinetics.

EXPERIMENTAL

The used experimental technique combines a conventional balanced-magnetron sputtering with independently generated arc discharge plasma that provides an independent control of the sputter-deposition and plasma immersion ion implantation. This capability allows ion current densities of $1 – 10\ mA{\cdot}cm^{-2}$ or higher for ion bombardment at the substrate independent of the sputtering rate. Ion-to-atom ratios of 0.1 – 10 ions/atom are achieved to tailor the microstructure of growing film. In the vacuum chamber (0.5 m in diameter and 1.2 m long) two cylindrical magnetrons (7.0 cm in diameter) symmet-rically surrounded the substrate holder that hosted samples $1 \times 1\ cm^2$ in size made of stainless steel (Alloy 600). The cathodes of magnetron were made of Mg and Al with a nominal purity better than 99.99 at.%. The gap distance between the cathode and sample was 7 cm. All samples were ultrasonically cleaned using acetone, then methanole.

*Corresponding author. Tel.: + 370-37-401909; fax: + 370-37-351271.
E-mail address: *milcius@mail.lei.lt* (D. Milčius)

The roughness was monitored by AFM and did not exceed 50 nm. The sample temperature during the deposition process was found to be an important parameter that affected the synthesis kinetics. Therefore, to ensure the accuracy of the temperature measurement, a thermocouple was connected to the rear side of sample holder.

A typical argon sputter-cleaning process was used to remove the surface contaminants and the residual oxide. A negative bias voltage of 100 V was applied to the sample holder. At the end of the sputter-cleaning process, after 15 min, the deposition of Mg atoms process proceeded without any interruption. During deposition, the pressure of the argon working gas was stabilized at pressure 0.2 Pa, and 500 W power on Mg magnetron was used. The magnetrons were switched out and the plasma immersion ion implantation was conducted when a typical thickness of approximately 2 – 4 μm was obtained (in approx. 10 min).

In plasma immersion ion implantation the sample is immersed in high-density plasma generated independently and is biased with a series of negative voltage pulses (0.5 – 1 kV). The supply of hydrogen was performed to keep the hydrogen working gas pressure equal to 10 Pa. The pulse repetition rate was kept fixed at 20 kHz, with the negative pulse duration equal to 10 μs. The principal characteristics of the plasma are as follows: plasma density $10^{10} – 10^{11}$ cm^{-3}, electron thermal temperature 0.5 – 1 eV, ion current to the sample 3 – 6 mA. The density of hydrogen atoms was less than 10 % of the molecular density. The ion density was 10^{-3} of the density of molecular hydrogen.

A "bias experiment" was undertaken to model the surface effects on the hydrogenation kinetics. The Mg samples are affected by the flux of hydrogen ions and charge exchange atoms with energies up to hundreds of eV and even several keV. These particles saturate the sample surface layer with hydrogen. It was performed by applying the negative bias voltage to the sample with respect to ground (which is very close to the plasma potential). Applying the bias potential leads to the modification of the surface state and to the change of the surface chemical potential. Thus we continuously supply the surface with hydrogen atoms and govern the surface thermodynamic properties due to structural and compositional perturbations of surface.

After the hydriding, the thin about 10 nm thick Al layer was deposited on the top of the film without interrupting the vacuum. Then the samples were removed from the chamber and subjected to the structural and properties analysis. After exposure of samples to air, thin 3 – 5 nm thick barrier layer of the natural oxide Al_2O_3 was formed on the surface which protected synthesized MgH_2 compound from the direct contact with air and moisture.

The microstructure of films was analyzed by X-ray diffraction (XRD, DRON 3) with the 2Θ angle in the range 20º – 90º using CuK_α radiation in steps of 0.05º. The average crystallite dimension of films, D, was calculated using the formula $D = 0.9\,\lambda\,(\beta\cos\Theta)^{-1}$ neglecting the microstrain, where λ is the X-ray wavelength, Θ is the Bragg diffraction angle and β is the full-width of the peak after correcting for the instrument broadening. The identification of phases has been performed using Crystallographica Search-Match program (Oxford Cryosystem Ltd, 1996-2003) based on Powder Diffraction Data. The scanning electron microscopy (SEM, JSM-5600) and atomic force microscopy (AFM, NT-206) were used for the studies of surface morphology and topography on all stages of film treatment.

The hydrogen release properties of the hydrogenated films were evaluated by using a thermal desorption technique. The hydrogen implanted films were put into the desorption cell, which was constructed by using standard stainless steel components. The desorption cell was installed at the inlet side of the glow discharge emission spectroscopy installation Spectrumat 1000 and equipped with a high resolution spectrometer. The flow of argon gas was used as a gas carrier for the desorbed hydrogen to be transported from the desorption cell into the plasma chamber of the Spectrumat. The turbomolecular pump (56 $\ell\cdot s^{-1}$) pumped continuously. The base pressure was less than 10^{-6} Pa. The argon pressure was equal to $2 – 5\cdot10^{-1}$ Pa. The parameters of the plasma were the following: discharge current – 10 mA, anode-cathode voltage – 1000 V, plasma density – $10^{10} – 10^{11}$ cm^{-3}, electron temperature – 0.1 – 0.5 eV and plasma volume – 15 cm^3. The samples were heated up to a temperature of 750 K. The given temperatures have been determined to be accurate within ±5 K. The temperature rise rate was equal to 18 ±0.1 K·min^{-1}.

RESULTS

Fig. 1 shows the XRD patterns of Mg film at different stages of the hydrogenation-dehydrogenation cycle. Before hydrogenation (Fig. 1, a), we can see Mg(002) and Mg(004) diffraction reflections. The relative intensity of the different peaks shows that magnesium growth is highly oriented along the c-axis. Structure of the as-deposited film can be modified changing the bias voltage. As the hydrogenation occurs, the Mg peaks diminish and the diffraction peaks corresponding to magnesium dehydride (MgH_2) at $2\Theta = 28°$, 36.5° and 40.5° appear in the diagram. With the increase in hydrogen concentration the MgH_2 peaks grow (Fig. 1, b and c). It is noteworthy, the measured positions of MgH_2 peaks are shifted to the database values 26.8°, 35.4° and 40.1°, respectively. This means that the lattice plane distance is changed and the MgH_2 phase may not swell to its equilibrium value. On the basis of the evolution of the amplitude of MgH_2 peaks in XRD patterns, the fractional volume of MgH_2 phase in the Mg film has been evaluated.

Fig. 2 includes the dependences the fractional volume of MgH_2 phase in Mg film on the hydrogenation duration for different sample temperatures. The shape of the curves shows that during the hydrogenation an incubation period of about 10 min for 450 K and 15 min for 400 K is followed by a fast formation of MgH_2 phase until the fraction volume of hydrogenated films reaches 0.9. Then the synthesis reaction rate decreases progressively and becomes very low. This shape is characteristic of a new phase nucleation and growth process. It is seen that the full transformation of Mg film into MgH_2 takes place after 35 min hydrogenation at 450 K, and after 65 min hydrogenation at 400 K.

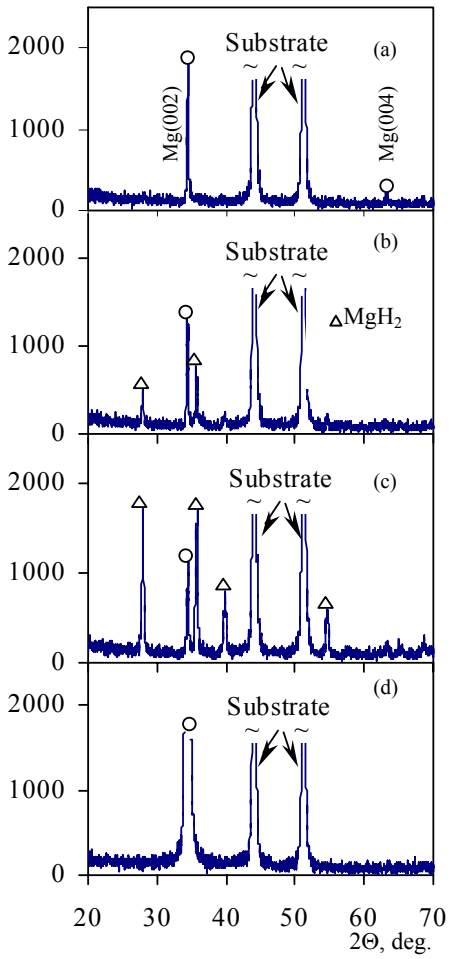

Fig. 1. XRD patterns of as-deposited Mg film (a), after 15 min hydriding at 450 K temperature (b) and 30 min hydriding at 450 K temperature (c) and after 15 min dehydriding at 520 K (d)

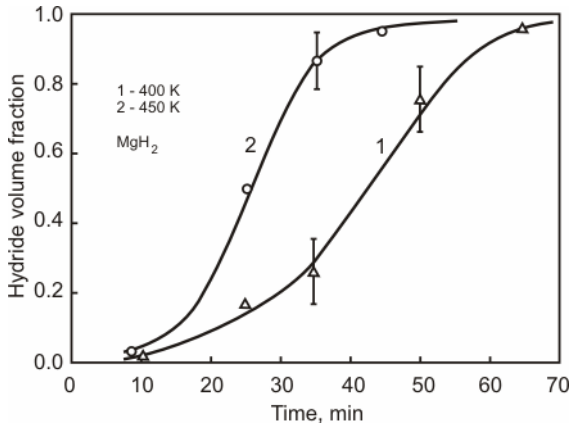

Fig. 2. Dependencies of the MgH_2 phase volume fraction in MgFilm on the hydriding duration for 400 K (curve 1) and 450 K (curve 2)

After dehydrogenation at 520 K for 15 min, the peaks corresponding to MgH_2 disappear as shown in Fig. 1, d profile and the peak corresponding to Mg(002) reflection appears. It is seen, the initial structure of the film is not restored. The peak of magnesium after the hydrogenation–dehydrogenation cycle becomes wider, indicating a decrease of the crystallite size. Using the Scherrer equation, the crystallite size is evaluated, within the experimental error, to vary from 46 nm for the initial Mg film to 28 nm after the dehydrogenation.

The residual stress values of hydrogenated samples are negative indicating a compressive stress. Considering the average crystallite size together, it is found that samples with larger crystallite size have lower residual stress. This may happen because for the larger crystallite size, there are fewer crystallite boundaries and dislocations, and thus lower residual stress.

The hydrogen effusion rate as a function of the sample temperature is included in Fig. 3. The hydrogenated at 480 K for 35 min Mg film presents a thermal desorption spectrum with a sharp effusion peak centered at about 530 K and small effusion peak centered at ~310 K (curve 1). The evaluations show that the total amount of the released hydrogen is about 10 % higher than the feasible amount of hydrogen stored in MgH_2 compound. It can be explained assuming that part of the hydrogen is located at grain boundaries of the nanocrystalline MgH_2 film. This excess is released at temperature ~310 K. The maximum efficiency of hydrogen effusion is observed at MgH_2 decomposition temperature, which is equal to 530 K [2]. For the partially hydrogenated Mg film when synthesis of MgH_2 is not complete, the main quantity of the released hydrogen is from grain boundaries. Curve 2 in Fig. 3 illustrates hydrogen effusion intensity for the Mg film hydrogenated at 450 K for 10 min (the fractional volume of MgH_2 in Mg film is about 0.1). It is seen that effusion curves included in Fig. 3 are the same qualitatively, however, they differ quantitatively: the quantities of hydrogen released from grain boundaries (low temperature effusion peaks at about 310 K) are about equal, and the quantities of hydrogen released after the thermal decomposition of MgH_2 compound (high temperature effusion peaks at about 530 K) are different.

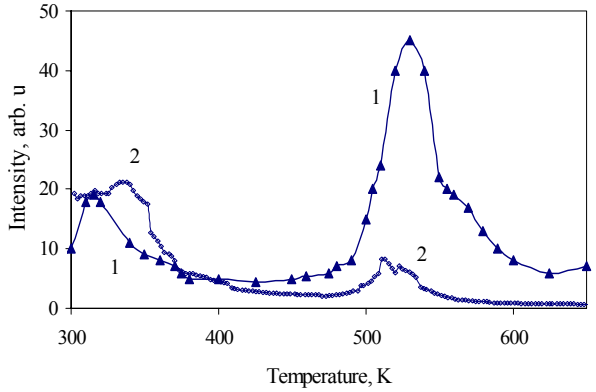

Fig. 3. Temperature dependencies of hydrogen effusion intensity for Mg film hydrogenated at 450 K for 30 min (curve 1) and at 450 K for 10 min (curve 2)

Fig. 4 shows the AFM images of Mg film as-deposited (a) and after the hydrogenation during 30 min for 450 K (b). It is seen that surface morphology of the as-deposited Mg film is controlled by nm-high growth mounds that have a characteristic length around 200 nm. Recent experiment and computational modeling [7, 8] have shown that the formation of growth mounds is produced by an asymmetry

in the attachment of atoms at ascending verses descending steps; this "diffusion bias" destabilizes the growth on low miscut surfaces. Surface irreguliarities produced by plastic deformations of Mg film become apparent for the hydrogenated Mg film (Fig. 4, b). In most cases, dislocation nucleation and glide appear to have occurred during hydrogenation since the morphologies are continuous across slip-steps. A slip-step formed should quickly initiate cracks and peeling. The formation of slip-step during the hydrogenation can be explained by the compressive stress in grain due to accommodation of adatoms at the interface between grain boundaries and the following plastic deformation of grain due to dislocation nucleation and glide [7].

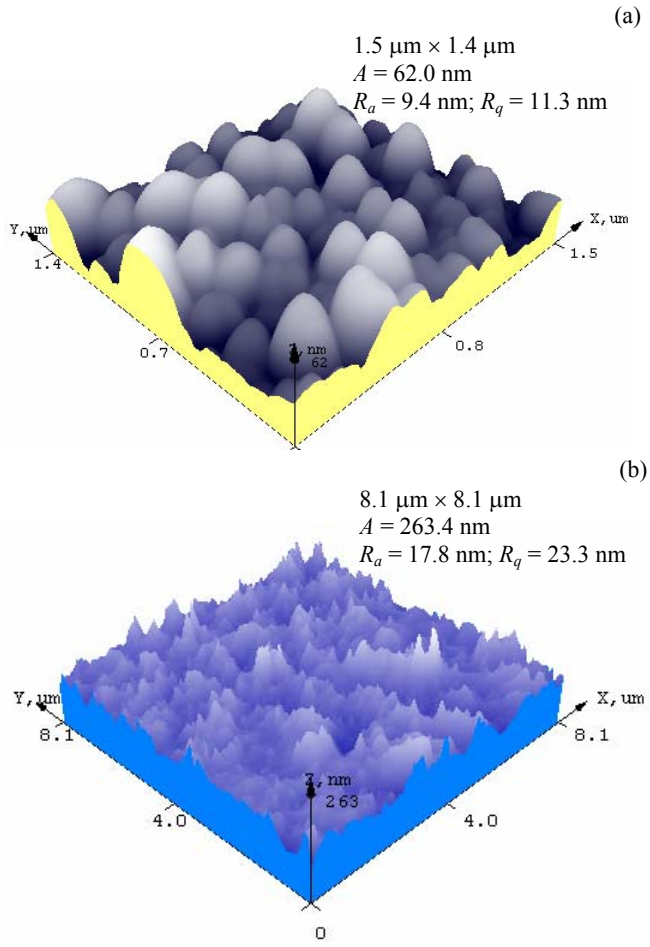

Fig. 4. AFM surfaces topography of the as-deposited Mg film (a) and after the hydrogenation at 450 K for 30 min (b)

AFM surface topography analysis shows that after the hydrogenation surface topography includes many well defined boundaries which are open and may serve as channels for the transportation of hydrogen from the surface into bulk and *vice versa*. These films have possibly a columnar, open and porous structure, which makes them transparent for hydrogen supplied through the surface.

DISCUSSIONS

The hydrogenation model is based upon the incorporation of excess of hydrogen atoms in grain boundaries during plasma immersion hydrogen ion implantation driven by the increase in surface chemical potential associated with the implantation flux. Surface irradiation effects increase the surface chemical potential through the formation of highly hydrogen saturated surface layer, the excess adatom population and activated their surface mobility [8]. The excess chemical potential of the surface relative to the grain boundary produces a net flux of hydrogen atoms from the very thin approximately equal to the penetration depth of incident ions (about 20 nm for 1 keV hydrogen ion energy) layer in the boundary that generates a compressive stress in the film [9]. The flow of hydrogen atoms will continue until the resultant compressive stress forces the chemical potential of the grain boundary to equal the chemical potential of the surface under intensive hydrogen irradiation, and steady state is achieved. The model relates the thin film hydrogenation kinetics directly to the irradiation process since origin is in the non-equilibrium nature of the irradiation activated surface.

The formation of highly hydrogen saturated thin surface layer under ion irradiation using 1 mA·cm^{-2} ion current density occurs during 2 – 3 s. The hydrogen atoms from it are driven into the grain boundaries. The grain interface boundary acts as a source for the diffusion of hydrogen into the bulk of grains.

The uptake of hydrogen through the grain boundaries in open contact with the highly hydrogen enriched surface occurs. Noteworthy, the net flow of hydrogen into the grain boundaries generates compressive stress in grains. If stress exceeds the limit of plasticity, the stress relaxation occurs through the emission of dislocations, the formation of subgrains within the original grain structure takes place. Initially grains form columnar well-textured microstructure, which is fragmented during hydrogenation and consists of nanocrystalline subgrains with the mean size equal to 20 – 40 nm. The high compressive stress in ion beam/plasma hydrogenated films is widely observed [10]. In many cases, hydrogenated film is peeled from the substrate. The hydrogen diffusion coefficient in stress activated grains can be 2 – 3 orders higher than the one in non-activated grains [11].

X-ray measurements show that the shift of diffraction peaks characteristic for the hydrogenated Mg film (Fig. 1, b) is related to compressive stress due to hydrogen incorporation within grain boundaries and not due to in the form of interstitials. This result provides additional support for the hypothesis of preferential grain-boundary incorporation.

The model predicts the reversible relaxation in the stress when the ion irradiation is terminated. Interruption of irradiation causes the surface potential to drop, and hydrogen atoms flow out of the grain boundary and back onto the surface, decreasing the stress and starting the hydrogen desorption process. Resumption of hydrogen ion irradiation reestablishes the enhanced surface potential, thereby reestablishing hydrogenation process, as observed.

The model explains the appearance of the low temperature desorption peak in H_2-effusion kinetics curve (Fig. 3), as the result of the release of weakly bonded hydrogen accommodated at grain boundaries. This flow of hydrogen is a thermal and is driven by stress relaxation process. The second peak in the H_2-effusion curve centered

at temperature 530 K (Fig. 3) is related to the release of bonded hydrogen accommodated in nanograins. After the thermal decomposition of chemical compound, the released hydrogen atoms diffuse to the grain boundaries and are transferred from bulk of the grains into the channels between grain boundaries forming the net flux of hydrogen driven to free surface.

The presented hydrogenation/dehydrogenation model is based on rudimentary assumption and simplified mechanics that makes quantitative predictions difficult. Compressive-stress generation due to hydrogen atom incorporation requires more extensive knowledge of how the surface chemical potential depends on irradiation parameters.

CONCLUSIONS

In this work, it has been shown that 2 μm thick Mg film is transformed into MgH_2 film under hydrogen plasma immersion ions implantation at 450 K for 15 min. All hydrogen desorbs at the temperature ~530 K which corresponds to the decomposition of $MgH_2 \rightarrow Mg + H_2\uparrow$. The macroscopic and microscopic observations show that magnesium film undergoes a high deformation during the hydrogenation-dehydrogenation reaction. This deformation is irreversible. The large number of defects created after hydrogenation ease the hydrogen release.

The important role of grain boundaries in the transport mechanism of hydrogen during the hydrogenation/dehydrogenation processes is emphasized when the uptake of hydrogen takes place through the grain boundaries in open contact with the highly hydrogen enriched surface layer. The driving forces of hydrogenation arise considering interaction between free surfaces, bulk and internal interfaces. The hydrogen ion irradiation increases the surface chemical potential, and dynamic behavior of adatoms forms highly hydrogen saturated layer on the surface. Under highly non-equilibrium conditions the difference in chemical potentials between the free surface layer and grain boundaries is established. It drives the hydrogen atoms from the surface into grain boundaries and creates high compressive stresses. At steady state, the balanced flux of hydrogen is directed from the bulk to the surface.

Acknowledgements

The work was performed under support from the Hydrogen Program of the US Department of Energy and the Sandia National Laboratories. The Lithuanian Science Foundation is gratefully acknowledged. The authors express their appreciation to Dr. Sandrock (USA) and Mr. A. Vasys (USA) for encouragement and kind cooperation to this work.

REFERENCES

1. **Sata, N., Eberman, K., Eberl, K., Maier, J.** Mesoscopic Fast Ion Conduction in Nanometre-Scale Planar Heterostructures *Nature* 408 2000: pp. 946 – 949.
2. **Leon, A., J. Knystautas, E., Hvot, J., Schulz, R.** Hydrogenation Characteristics of Air-Exposed Magnesium Films *J. Alloys Comp.* 345 2002: pp. 158 – 166.
3. **Majbouz, E. H., Gross, K. J.** Titanium-halide Catalyst-Precursors in Sodium Aluminium Hydrides *J. Alloys Comp.* 356 – 357 2003: pp. 363 – 367.
4. **Bouaricha, S., Dodelet, J. P., Guary, D., Huot, J., Schultz, R.** Activation Characteristics of Graphite Modified Hydrogen Absorbing Materials *J. Alloys Comp.* 325 2001: pp. 245 – 251.
5. **Zaluska, A., Zaluski, L., Strom-Olsen, J. O.** Nanocrystalline Magnesium for Hydrogen Storage *J. Alloys Comp*. 288 1999: pp. 217 – 225.
6. **Huot, J., Liang, G., Boily, S., Van Neste, A., Schultz, R.** Structural Study and Hydrogen Sorption Kinetics of Ball-Milled Magnesium Hydride *J. Alloys Comp*. 293 – 295 1999: pp. 495 – 500.
7. **Pranevicius, L., Milcius, D., Pranevicius, L. L., Templier, C., Sirvinskaite, V., Knizikevicius, R.** Role of Surface Instabilities in Mixing and Oxidation Kinetics of Bilayered Y/Zr Films at Elevated Temperature *Applied Surface Science* 225 2004: pp. 272 – 280.
8. **Pranevicius, L., Milcius, D., Pranevicius, L.L., Thomas, G.J.** Plasma Hydrogenation of Al, Mg and MgAl Films under High-Flux Ion Irradiation at Elevated Temperature *J. Alloys Comp.* 373 2004: pp. 9 – 15.
9. **Floro, J. A., Chason, E., Cammarata, R. C., Slovitz, D.** Physical Origins of Intrinsic Stresses in Volmer-Weber Thin Films *MRS Bulletin January* 2002: pp. 19 – 25.
10. **Huot, J., Pelletier, J.F., Liang, G., Sulton, M., Schultz, R.** Structure of Nanocomposite Metal Hydrides *J. Alloys Comp.* 330 – 332 2002: pp. 727 – 731.
11. **Randall, N. X., Renevier, N., Michel, H., Colligon, P.** Correlation Between Processing Parameters and Mechanical Properties *Vacuum* 48 1997: pp. 849 – 855.

DOI: 10.5755/j02.ms.26523